DTIC FILE COPY

(1)

AD-A202 693

DTIC
ELECTE
JAN 18 1989
S D
cb H

DEPARTMENT OF THE AIR FORCE

AIR UNIVERSITY

AIR FORCE INSTITUTE OF TECHNOLOGY

Wright-Patterson Air Force Base, Ohio

DISTRIBUTION STATEMENT A
Approved for public release;
Distribution Unlimited

89 1 17 034

AFIT/GA/AA/88D-7

OPTIMAL LAUNCH TIME FOR A DISCONTINUOUS LOW THRUST ORBIT TRANSFER

THESIS

Jeffrey M. McCann
Captain, USAF

AFIT/GA/AA/88D-7

DTIC
ELECTE
JAN 18 1989
S D
H

Approved for public release; distribution unlimited

AFIT/GA/AA/88D-7

OPTIMAL LAUNCH TIME FOR A DISCONTINUOUS LOW THRUST ORBIT TRANSFER

THESIS

Presented to the Faculty of the School of Engineering
of the Air Force Institute of Technology
Air University
In Partial Fulfillment of the
Requirements for the Degree of
Master of Science in Astronautical Engineering

Jeffrey M. McCann, B.S.
Captain, USAF

December 1988

Approved for public release; distribution unlimited

Preface

Electric propulsion is a viable alternative to chemical propulsion for orbit transfers. The difference between present day chemical rockets and the near term electric rockets is similar to the difference between a Lamborghini Countach and a moped. Both will get you to where you want to go but the moped is much more efficient and considerably slower. Electric rockets could be the moped of transfer vehicles.

Electric propulsion will improve the cost efficiency for payloads, thereby making this endeavor more profitable. As budget constraints mount, the space industry must look for more cost efficient, yet safe, systems for deploying payloads to various orbits. Electric rockets may be the solution to this system search. However, this solution hinges on one notion: transfer time is not important. The slogan for a NASA/USAF/industry electric rocket could be: if you've got the time, we've got the rocket.

I would like to thank my advisor Dr. William Wiesel for introducing me to this up and coming technology and for his patience during my learning curve. I would also like to thank my committee members Capt James Planeaux and Capt Rodney Bain. A special thanks is due to Capt Bain for his advise and guidance while I was a part-time AFIT student prior to my full-time acceptance.

Table of Contents

COPY INSPECTED

Accession For
NTIS GRA&I
DTIC TAB
Unannounced
Justification
By
Distribution/
Availability Codes
Dist | Avail and/or Special
A-1

List of Figures

List of Tables

List of Symbols

a	semi-major axis
B	orbital latitude of the anti-sun point
DU	distance unit (6378 km or 2.092567×10^7 ft)
e	eccentricity
f	true anomaly
F_o	earth-sun related constant
g	angle between shadow exit point and next shadow entry
G	universal gravitation constant
G_o	earth-sun related constant
H	Hamiltonian
i	orbital inclination
J	performance index
L	position angle of anti-sun point
m	one-half actual shadow angle
m_o	one-half actual shadow angle at initial conditions
$\dot{m}_p$	specific mass flow rate
$M_\oplus$	mass of the earth
n	mean motion
$R_\odot$	angular semi-diameter of the sun
s	angle between ascending node and shadow exit point
t	time
T	total acceleration
T_o	initial T
TU	time unit (806.8 seconds) (2:429)
u	control variable ($u = \lambda_1 a$)

U radial acceleration

V tangential acceleration

W normal acceleration

α thrust angle in orbit plane

$\alpha_{\odot}$ right ascension of the sun

$\delta_{\odot}$ declination of the sun

γ thrust angle out of orbit plane

λ_a Lagrange multiplier for minimum time solution

λ_i Lagrange multiplier for minimum time solution

λ_1 Lagrange multiplier for optimal control law

λ_2 Lagrange multiplier for optimal control law

μ gravitational parameter

ω argument of perigee

Ω longitude of the ascending node

π_s parallax of the satellite

$\pi_{\odot}$ parallax of the sun

σ_o one-half of the maximum shadow angle

τ total accumulated velocity change

Abstract

This study searches for the optimal launch time of a discontinuous, low thrust transfer between non-coplanar, circular orbits. The spacecraft is assumed to be a solar-powered rocket that cannot provide thrust in the earth's shadow.

Two timescales are used to calculate a minimum time trajectory. The fast timescale produces a control law which maximizes a change in orbital elements for a single orbit. The slow timescale incorporates the control law so that the final boundary conditions are met in minimum time. Minimum transfer times are determined between winter and summer.

OPTIMAL LAUNCH TIME FOR A DISCONTINUOUS, LOW THRUST, ORBIT TRANSFER

I. INTRODUCTION

The orbit transfer condsidered in this study is between a 200 km circular orbit ($a \approx 1.03$ DU) with an inclination of 28.5 degrees and a geosynchronous orbit ($a \approx 6.6$ DU). The launch time is broken into two components: time of day (i.e., ascending node) and time of year. The optimal launch time is determined by minimizing the transfer time. Discontinuous low thrust is possible using a certain type of electric propulsion. An overview of electric propulsion is given below.

Propulsion systems may be classified into two basic categories:

1. Endogenous, which use energy stored within the propellants to create thrust. Solid rockets and liquid rockets are common examples of endogenous systems.

2. Exogenous, in which the energy is supplied to the propellant from an outside power source. All electric propulsion systems are exogenous, although some can be a combination of the two.

The most significant advantage of an exogenous system is that, if external energy is available for accelerating a propellant, the resulting specific impulse can be much more than that of an endogenous system. For example, an ion

thruster system with a specific impulse of 3000 seconds would require only 2000 kg of ion propellant as compared to 15,000 kg of chemical propellant for a liquid oxygen-liquid hydrogen upper stage rocket with the same total impulse. The dry weights of the two systems are also similar, resulting in a significant advantage for the ion thruster system (7:xii).

Electric propulsion devices are low thrust devices. This allows very fragile large space structures to be transported from low earth orbit to geosynchronous orbit. In addition, since the propellant is a small fraction of the overall system mass, weight growth of the payload during the construction phase of the project can easily be accommodated by thrusting for a longer period of time (7:xiii). Payload mass is not a constraint as in chemical systems, it merely requires longer transfer times. Other benefits include better cost efficiency (lower dollar/kg of payload) and less complex engine design.

There are three classes of electric propulsion devices, all of which are capable of high specific impulse.

1. Electromagnetic. The electromagnetic thruster is often called the plasma thruster. In this thruster, the propellant gas is ionized to form a plasma, which is then accelerated rearward by electric and magnetic fields.

2. Electrostatic. The best known type of electrostatic thruster is the ion thruster. As in the plasma thruster, propellant atoms are ionized by removing an electron from each atom. In the electrostatic thruster, however, the

electrons are removed from the ionization region at the same rate as ions are accelerated rearward.

3. Electrothermal. The electrothermal thruster is the thruster which fueled this study. In this thruster, electric power or solar radiation is used to heat the propellant to a high temperature. The heating may be done by producing an electric discharge through the propellant gas (arcjet) or by flowing the propellant gas over surfaces heated using electricity (resistojet) or reflected sunlight. If reflected sunlight is used to heat the propellant, then this would result in discontinuous low thrust. Discontinuous because the spacecraft might enter the earth's shadow during an orbit (3:1-9, 7:xiii-xvi).

A discontinuous, low-thrust orbit transfer between two non-coplanar, circular orbits may soon be accomplished by a spacecraft currently being developed at the Air Force Astronautics Laboratory. The spacecraft is a solar-powered rocket capable of transferring large payloads from low earth orbit to geosynchronous orbit. The booster will likely employ two solar collectors which concentrate reflected sunlight and focus it to an area on the engine. The hydrogen propellant is heated and then expelled through a nozzle. Using solar-heated liquid hydrogen as the propellant, the low thrust, high specific impulse engine may evolve into an efficient powerplant for space transportation by the end of the century (11:119-120).

The concept of a solar powered boost vehicle is not new.

The current Air Force development program is an outgrowth of solar engine research that originated in the early 1960's (11:119). The revival of this concept is brought about by new materials and new control techniques for the solar collectors. A solar powered booster could be an important component in the USAF space inventory.

Previous work on low thrust transfers between non-coplanar circular orbits revealed an outward spiral is the optimal trajectory (1,6:1, 10:150-154). Cass later derived a control law for a discontinuous, low thrust transfer between non-coplanar circular orbits (6:18). That is, a constraint was added such that the eccentricity equals zero. This study was conducted to locate the optimal launch time by minimizing transfer time using the control law derived by Cass.

The derivation is divided into two problems of differing timescales. The fast timescale problem optimizes the changes in the semi-major axis and inclination over one orbit with vehicle mass held constant. The result is an optimal control law for one orbit. The slow timescale problem uses the optimal control law to determine how much to change the semi-major axis and inclination on each orbit so that the final boundary conditions are met in minimum time. The mass and acceleration are updated after each orbit.

II. DERIVATION

A control law was previously derived by Cass for the discontinuous low thrust orbit transfer problem(6). The purpose of this study is to use the control law to find the optimal launch time. The optimal launch time minimizes transfer time. To avoid duplication of effort, Cass's work will not be rederived. However, the pertinent concepts, equations, and optimization algorithm will be fully described.

The derivation was divided into two problems of differing timescales; the fast timescale and the slow timescale. The fast timescale problem optimizes the changes in semi-major axis and inclination during one orbit of the central body (earth) with vehicle mass held constant. The slow timescale problem incorporates the fast timescales results and determines how much to change the semi-major axis and inclination on each orbit so that the final boundary conditions are reached in minimum time. Vehicle mass was recomputed after each orbit to account for propellant loss.

FAST TIMESCALE PROBLEM (6:3-18)

The solution of the fast timescale problem will yield the optimum thrust control law for one orbit. The thrust control law maximizes a change in either inclination or semi-major axis when a particular change in the other is specified. The derivation assumes two-body motion with the earth as the

central body. Also, since electric engines produce low thrust, the change in orbital elements for one orbit is assumed to be very small (i.e., $da \approx \Delta a$). Therefore, the orbital elements are considered constant during each orbit. The spacecraft mass is also considered constant for one orbit since propellant loss is very small.

Lagrange's planetary equations in their acceleration component form are used to find the optimal thrust control law. The planetary equations are (12:35):

$$\frac{d\Omega}{dt} = \frac{W\ (1-e^2)^{1/2}\ \sin(\omega+f)}{n\ a\ \sin(i)\ (1 + e\ \cos(f))} \tag{1}$$

$$\frac{di}{dt} = \frac{W\ (1-e^2)^{1/2}\ \cos(\omega+f)}{n\ a\ (1 + e\ \cos(f))} \tag{2}$$

$$\frac{d\omega}{dt} = \frac{-U\ (1-e^2)^{1/2}\ \cos(f)}{n\ a\ e} - \frac{W\ (1-e^2)^{1/2}\ \cot(i)\ \sin(\omega + f)}{n\ a\ (1 + e\ \cos(f))}$$

$$+ \frac{V\ (1-e^2)^{1/2}\ \sin(f)\ (2 + e\ \cos(f))}{n\ a\ e\ (1 + e\ \cos(f))} \tag{3}$$

$$\frac{de}{dt} = \frac{U\ (1-e^2)^{1/2}\ \sin(f)}{n\ a}$$

$$+ \frac{V\ (1-e^2)^{1/2}}{n\ a\ e}\left[1 + e\ \cos(f) - \frac{(1-e^2)}{1+e\ \cos(f)}\right] \tag{4}$$

$$\frac{da}{dt} = \frac{2\,U\,e\,\sin(f)}{n\,(1-e^2)^{1/2}} + \frac{2\,V\,(1+e\,\cos(f))}{n\,(1-e^2)^{1/2}} \qquad (5)$$

where Ω is the longitude of the ascending node, ω is the argument of perigee, i is the spacecraft inclination, e is the orbit eccentricity, a is the semi-major axis, and f is the true anomaly. These orbital elements are shown in Figure 1. The variables U,V, and W are the radial, tangential, and normal acceleration component, respectively, and n is the mean motion which is given by:

$$n = (\mu/a^3)^{1/2} \qquad (6)$$

where

$$\mu = G\,M_{\oplus} \qquad (7)$$

and G is the universal gravitation constant and $M_{\oplus}$ is the mass of the earth.

For this problem, the initial and final orbits are defined to be circular (e = 0). In addition to these boundary conditions, the eccentricity for each orbit is set equal to zero throughout the entire orbit transfer. That is, a constraint is introduced which requires the change in eccentricity between each orbit be equal to zero. This constraint greatly simplifies the planetary equations, as shown below:

$$\frac{d\Omega}{dt} = \frac{W\,\sin(\omega+f)}{n\,a\,\sin(i)} \qquad (8)$$

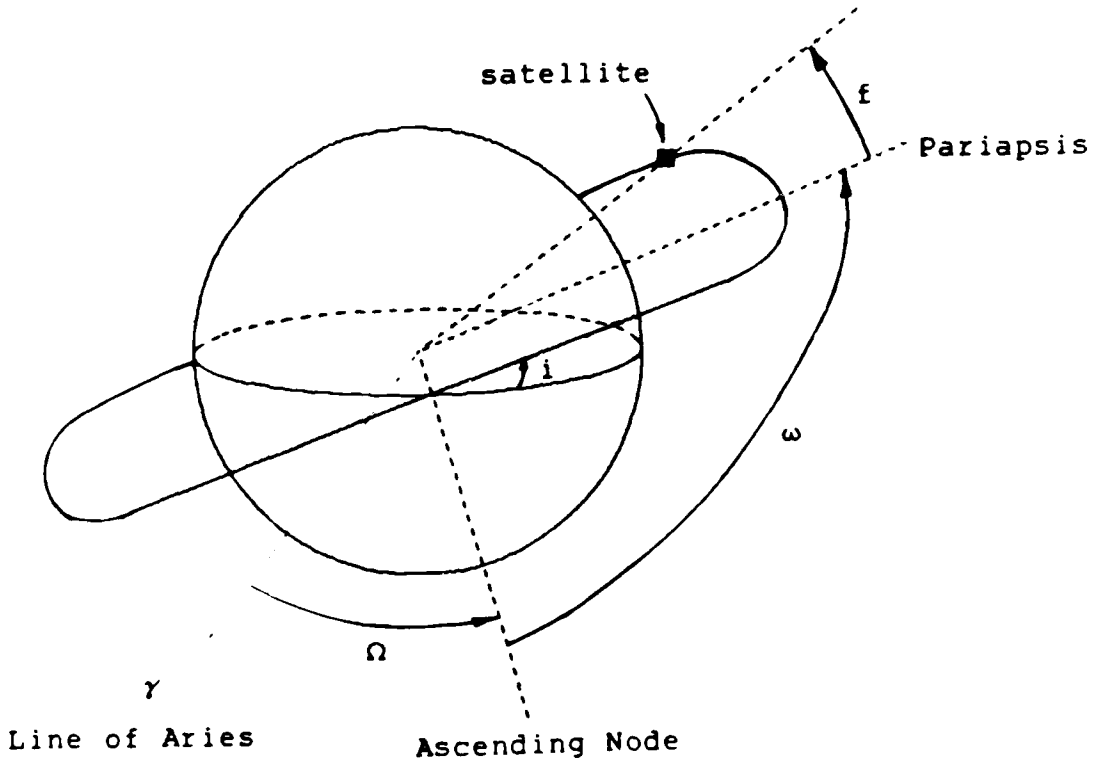

Figure 1. Orbital Elements

$$\frac{di}{dt} = \frac{W \cos(\omega+f)}{n\ a} \tag{9}$$

$$\frac{d\omega}{dt} = \text{undefined for a circular orbit} \tag{10}$$

$$\frac{de}{dt} = \frac{U \sin(f)}{n\ a} + \frac{2\ V \cos(f)}{n\ a} \tag{11}$$

$$\frac{da}{dt} = \frac{2\ V}{n} \tag{12}$$

In general, ω is undefined for a circular orbit. Thus, the new reference point for f is the ascending node as shown in Figure 1. For continuous thrust vehicles, f is the vehicle's angular displacement with the engines on. In this problem, thrust is possible only in the sunlight. Accordingly, angle f is redefined as the angular displacement of the spacecraft in the sunlight measured with respect to the earth's shadow exit point. A new angle, s, is introduced to give the angular displacement between the ascending node and the shadow exit point. Now, there is a complete definition of the spacecraft's position with respect to the ascending node as shown in Figure 2. Thus, the angle $(\omega+f)$ in Eqs (8) and (9) is replaced by $(s+f)$. Also, the angle g is measured between the shadow exit to the next shadow entry

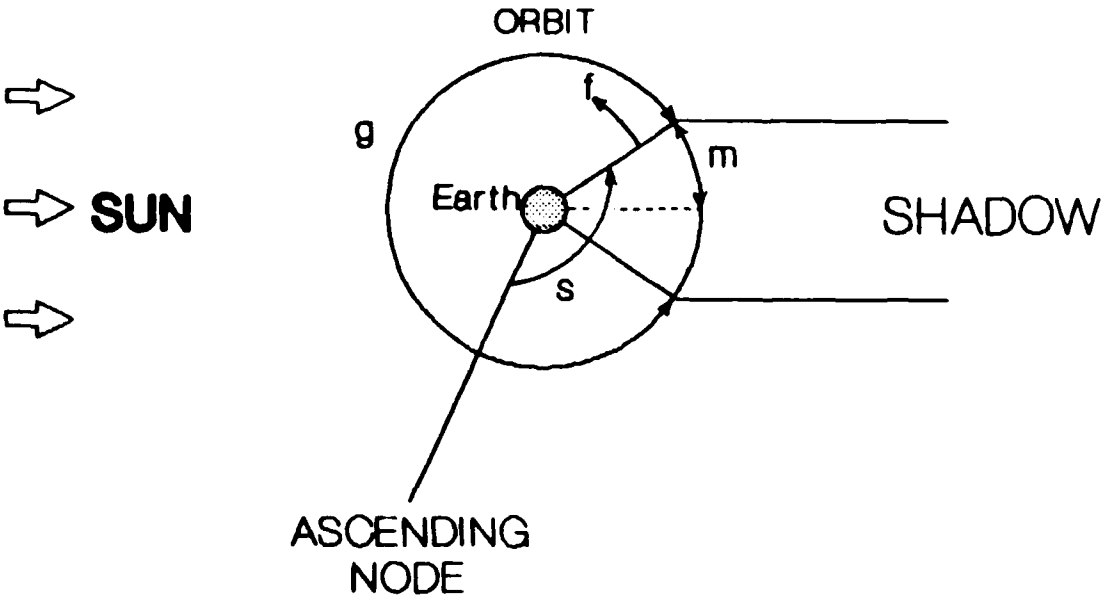

Figure 2. Shadow-Related Angles

and m is one-half of the shadow angle. See Figure 2 for a depiction of these angles. Uses of angles g and m are discussed later in this section.

Additional modifications to the planetary equations include changing the independent variable from t to f (using $n = df/dt$) and replacing n with $(\mu/a^3)^{1/2}$ (Eq (6)). The planetary equations are now:

$$\frac{d\Omega}{df} = \frac{W\, a^2 \sin(f+s)}{\mu \sin(i)} \tag{13}$$

$$\frac{di}{df} = \frac{W\, a^2 \cos(f+s)}{\mu} \tag{14}$$

$$\frac{de}{df} = \frac{a^2}{\mu} \left[U \sin(f) + 2\, V \cos(f)\right] \tag{15}$$

$$\frac{da}{df} = \frac{2\, V\, a^3}{\mu} \tag{16}$$

To determine the changes in the orbital elements for one orbit, Eqs (13) through (16) should be integrated from 0 to 2π; but U, V, and W are zero when the vehicle is in the earth's shadow. Therefore, these equations are integrated from 0 to g, where g is measured from the shadow exit to the next shadow entry.

$$g = 2\pi - 2m = 2(\pi - m) \tag{17}$$

where m is one-half of the shadow angle(see Figure 2).

The accelerations U, V, and W are modeled as functions of f. From Figure 3:

$$U = T \cos\gamma \cos\alpha \tag{18}$$

$$V = T \cos\gamma \sin\alpha \tag{19}$$

$$W = T \sin\gamma \tag{20}$$

where

$$\gamma = \gamma(f) \tag{21}$$

$$\alpha = \alpha(f) \tag{22}$$

and T is the total acceleration due to the thrust. Substituting Eqs (18) through (20) into Eqs (13) through (16) and integrating between 0 and g, the change in orbital elements become:

$$\Delta\Omega \approx d\Omega = \frac{T\, a^2}{\mu \sin(i)} \int_0^g \sin(\gamma) \sin(f+s)\ df \tag{23}$$

$$\Delta i \approx di = \frac{T\, a^2}{\mu} \int_0^g \sin(\gamma) \cos(f+s)\ df \tag{24}$$

$$\Delta e \approx de = \frac{T\, a^2}{\mu} \int_0^g (\cos(\gamma) \cos(\alpha) \sin(f) + 2 \cos(\gamma) \sin(\alpha) \cos(f))\ df \tag{25}$$

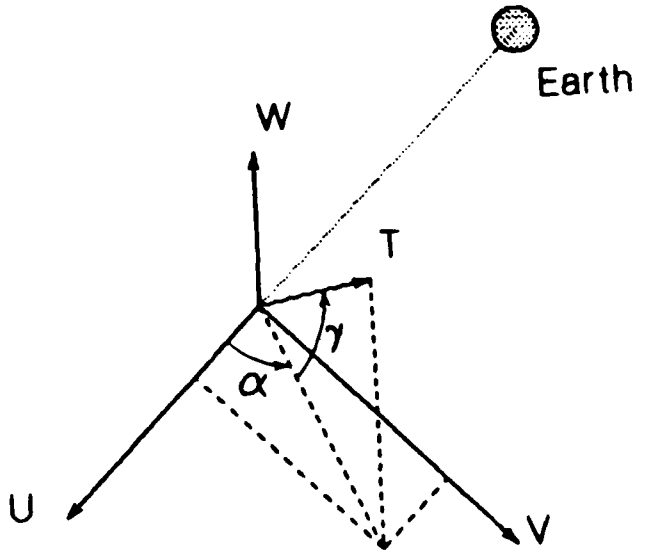

Figure 3. Acceleration Components

$$\Delta a \approx da = \frac{2\ T\ a^3}{\mu} \int_o^g \cos(\gamma)\ \sin(\alpha)\ \ df \tag{26}$$

The following conditions are used to find the optimal thrust control law for one orbit: Δi is maximized for a given Δa, subject to the constraint $\Delta e = 0$. The performance index with constraint relationships is:

$$J(\alpha,\gamma) = \int_o^g \frac{T\ a^2}{\mu}\ \sin(\gamma)\ \cos(f+s)\ \ df$$

$$+\ \lambda_1 \left[\int_o^g \frac{2\ T\ a^3}{\mu} \cos(\gamma)\ \sin(\alpha)\ \ df \ -\ \Delta a \right]$$

$$+ \lambda_2 \int_o^g \frac{T\ a^2}{\mu}(\cos(\gamma)\ \cos(\alpha)\ \sin(f) + 2\cos(\gamma)\ \sin(\alpha)\ \cos(f))\ df \tag{27}$$

where λ_1 and λ_2 are Lagrange multipliers. The goal is to find the functions γ and α that produce a stationary value of J. The solution of this problem was done by Cass and is patterned after an optimization scheme given by Bryson and Ho (4:48-49). The optimal thrust control law is:

$$\alpha = \tan^{-1}\left[\frac{2(\lambda_1 a + \lambda_2 \cos(f))}{\lambda_2\ \sin(f)}\right] \tag{28}$$

$$\gamma = \tan^{-1}\left[\frac{\cos(f+s)}{[\lambda_2^2\ \sin^2(f) + 4(\lambda_1 a + \lambda_2 \cos(f))^2]^{1/2}}\right] \tag{29}$$

Substituting Eqs (28) and (29) into Eqs (24) through (26) yields:

$$\Delta i = \frac{T\,a^2}{\mu} \int_o^g \frac{\cos^2(f+s)\quad df}{[\lambda_2^2 \sin^2(f) + 4(\lambda_1 a + \lambda_2 \cos(f))^2 + \cos^2(f+s)]^{1/2}} \tag{30}$$

$$\Delta e = \frac{T\,a^2}{\mu} \int_o^g \frac{[\lambda_2 \sin^2(f) + 4\cos(f)\,(\lambda_1 a + \lambda_2 \cos(f)]\,df}{[\lambda_2^2 \sin^2(f) + 4(\lambda_1 a + \lambda_2 \cos(f))^2 + \cos^2(f+s)]^{1/2}} \tag{31}$$

$$\Delta a = \frac{4\,T\,a^3}{\mu} \int_o^g \frac{[\lambda_1 a + \lambda_2 \cos(f)]\quad df}{[\lambda_2^2 \sin^2(f) + 4(\lambda_1 a + \lambda_2 \cos(f))^2 + \cos^2(f+s)]^{1/2}} \tag{32}$$

Assuming a sperical earth, $\Delta\Omega$ is neglected and will not be considered in this problem. For convenience, let:

$$u = \lambda_1 a \tag{33}$$

and

$$D = \lambda_2^2 \sin^2(f) + 4(u + \lambda_2 \cos(f))^2 + \cos^2(f+s). \tag{34}$$

Substitution yields:

$$\Delta i = \frac{T\, a^2}{\mu} \int_o^g \frac{\cos^2(f+s)\quad df}{D^{1/2}} \tag{35}$$

$$\Delta e = \frac{T\, a^2}{\mu} \int_o^g \frac{[\lambda_2 \sin^2(f) + 4\cos(f)\ (u + \lambda_2 \cos(f))]\ df}{D^{1/2}} \tag{36}$$

$$\Delta a = \frac{4\ T\ a^3}{\mu} \int_o^g \frac{[u + \lambda_2 \cos(f)]\quad df}{D^{1/2}} \tag{37}$$

Eqs (35) through (37) represent changes in i, e, and a for one orbit using the optimal thrust control law. Actually, this control law will maximize Δi for a given Δa, subject to the constraint $\Delta e = 0$. Eqs (35) and (37) will be used in the slow timescale problem to ensure optimal control during each orbit and to define the amount of change possible for Δi and Δa on a given orbit. The $\Delta e=0$ constraint is solved numerically to determine u and λ_2(further use of Eq (36) is given in the next section).

However, before these equations are implemented the angles m and s must be calculated. Recall m is one-half of the shadow angle and s is an angle in the orbit plane between the ascending node and the point where the spacecraft exits the earth's shadow. Sun-earth geometrical relationships are used to determine m and s. According to Link (9:122-127),

the following sun-earth geometrical relationships are used to calculate m (see Figure 4):

$$\cos(m) = \frac{\cos(\sigma_o)}{\cos(B)} \tag{38}$$

where B and σ_o are angles shown in Figures 4 and 5 and σ_o is half of the maximum shadow possible for a given altitude. Link also gives expressions for the angles B and σ_o:

$$\cos(B) = [1 - (\cos(\delta_\odot)\sin(i)\sin(\alpha_\odot-\Omega) - \sin(\delta_\odot)\cos(i))^2]^{1/2} \tag{39}$$

and

$$\sigma_o = \pi_\odot + \pi_* - R_\odot \tag{40}$$

or

$$\cos(\sigma_o) = F_o\,[1 - a^{-2}]^{1/2} + [G_o/a] \tag{41}$$

where $\alpha_\odot$ and $\delta_\odot$ are the right ascension and declination of the sun in earth centered coordinates and F_o and G_o are constants depending on the size of the earth and sun and the distance between them.

$$F_o = 0.99994668 \qquad G_o = 0.0046229536$$

Link also has an expression for s:

$$s = (\pi/2) - L + m \tag{42}$$

where

$$L = -\cos(\alpha_\odot-\Omega)\,\frac{\cos(\delta_\odot)}{\cos(B)} \tag{43}$$

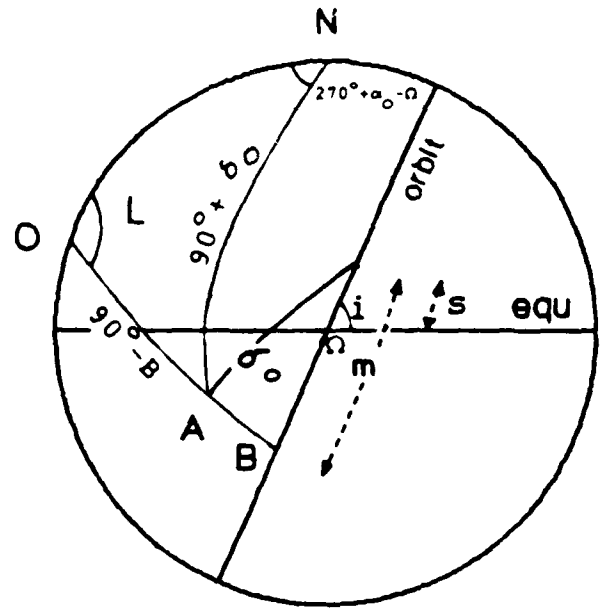

Figure 4. Ephemeris of the Eclipse

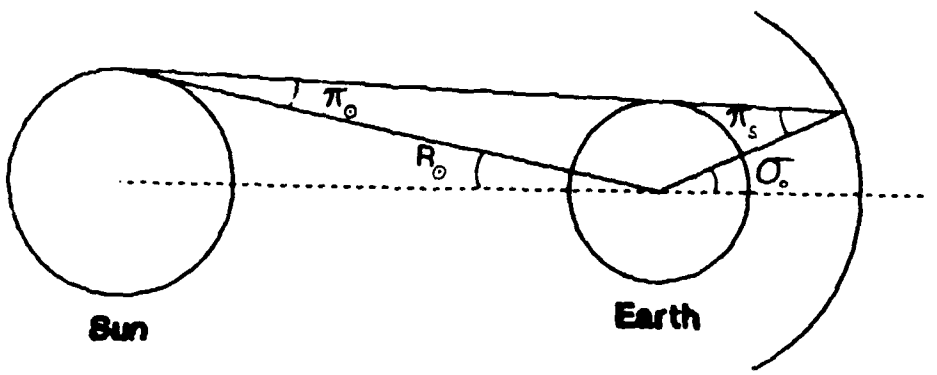

Figure 5. Sun-Earth Shadow Geometry

All ingredients should now be available for the slow timescale problem.

SLOW TIMESCALE PROBLEM (6:26-37)

The purpose of solving the slow timescale problem is to determine how much to change the semi-major axis and inclination on each orbit such that final boundary conditions are met in minimum time. Fast timescale results for Δa, Δi, and Δe are used to ensure optimal control during each orbit and to define the amount of change possible for Δa and Δi on a given orbit. Mass is recomputed for each orbit to compensate for propellant loss.

Before the minimum time control problem is solved, a few preliminary steps are taken. An expression is needed for da/dt and di/dt for the slow timescale problem. Since the orbital elements change very little on each orbit, these rates are approximated by:

$$\frac{da}{dt} \approx \frac{\Delta a}{\Delta t} \tag{44}$$

$$\frac{di}{dt} \approx \frac{\Delta i}{\Delta t} \tag{45}$$

where Δt is the orbital period. For a circular orbit,

$$\Delta t = 2\pi \left[a^3/\mu\right]^{1/2}. \tag{46}$$

However, the elements a and i only change when the spacecraft is in sunlight. Therefore, Δt must be altered to only cover

that portion of the orbit. The new Δt is:

$$\Delta t = \frac{g}{2\pi} \text{ (orbital period)} = 2(\pi - m)[a^3/\mu]^{1/2} \qquad (47)$$

Dividing Eqs (35) and (37) by Δt yields:

$$\frac{da}{dt} = \frac{2\,T\,a^{3/2}}{\mu^{1/2}\,(\pi - m)} \int_o^g \frac{(u + \lambda_z \cos(f)\ \ df}{D^{1/2}} \qquad (48)$$

$$\frac{di}{dt} = \frac{T\,a^{1/2}}{2\mu^{1/2}\,(\pi - m)} \int_o^g \frac{\cos^2(f+s)\ \ df}{D^{1/2}} \qquad (49)$$

Since the goal is to find a minimum thrusting time, only the time in which the spacecraft is in the sunlight is considered. The total thrusting time for the entire orbit transfer is the summation of <u>thrusting</u> time for each orbit.

As previously stated, the spacecraft's mass is recomputed for each orbit to account for propellant loss. The propellant loss causes an increase in acceleration. For a constant thrust ion rocket, propellant flow is constant. Acceleration can be modeled as a function of time:

$$T(t) = \frac{T_o}{1 - \dot{m}_p t} \qquad (50)$$

where T_o is the initial spacecraft acceleration, t is the time, and $\dot{m}_p$ is the specific mass flow rate(mass flow rate

divided by initial spacecraft mass).

Eqs (48) and (49) can be solved more easily if there is no time dependence. To eliminate the time dependence, a change of variable is made. The new independent variable τ is defined by:

$$d\tau = T(t)\ dt = \left[\frac{T_o}{1 - \dot{m}_p\ t} \right] dt \qquad (51)$$

where τ is the total accumulated velocity change. The units of τ are DU/TU. Minimizing τ will minimize the thrusting time and fuel expended. Using τ as the independent variable will not yield the number of orbits and total thrusting time (in seconds) when the final boundary conditions are met. These values depend on the engine performance parameters (T_o, $\dot{m}_p$,etc...). The solution using τ as the independent variable will give the change in velocity needed to reach the final boundary conditions for any type of low thrust engine. By integrating Eq (51), an expression relating the engine performance parameters and time to τ is found. With $\tau = 0$ when $t = 0$

$$\tau = -(T_o / \dot{m}_p)\ \ln (1 - \dot{m}_p\ t) \qquad (52)$$

Substituting Eq (51) into Eqs (48) and (49) gives:

$$\frac{da}{d\tau} = \frac{2\ a^{3/2}}{\mu^{1/2}\ (\pi-m)} \int_0^g \frac{(u + \lambda_2 \cos(f))\ \ df}{D^{1/2}} \tag{53}$$

$$\frac{di}{d\tau} = \frac{a^{1/2}}{2\mu^{1/2}\ (\pi-m)} \int_0^g \frac{\cos^2(f+s)\ \ df}{D^{1/2}} \tag{54}$$

Eqs (53) and (54) are essential in finding the minimum time solution. Cass provides the derivation to the minimum time problem using the minimum time solution given in Bryson and Ho (4:87-89).

Bryson and Ho have shown a minimum time solution satisfies the following three conditions:

$$H(t_f) = 0 \tag{55}$$

$$\frac{\partial H}{\partial u_k} = 0 \qquad k = 1,2,3,\ldots,r \tag{56}$$

$$\lambda_j' = \frac{-\partial H}{\partial x_j} \qquad j = 1,2,3,\ldots,q \tag{57}$$

where H is the Hamiltonian, λ_j's are Lagrange multipliers, x_j's are the state variables, and the u_k's are the control variables. The prime indicates differentiation with respect to τ. In this problem, $r = 1$ ($u_1 = u$) and $q = 2$ ($x_1 = a$ and $x_2 = i$). Eqs (55) through (57) will now be applied to this specific problem.

For this problem, the Hamiltonian is

$$H = \lambda_a \frac{da}{d\tau} + \lambda_i \frac{di}{d\tau} + 1 \qquad (58)$$

Since t does not appear explicitly in H,

$$\dot{H} = 0 \qquad (59)$$

Therefore, $H(t_f) = 0$ implies

$$H(t) = 0 \qquad (60)$$

for all $t \geq 0$. So Eq (58) becomes

$$\lambda_a \frac{da}{d\tau} + \lambda_i \frac{di}{d\tau} + 1 = 0 \qquad (61)$$

for all time. Substituting Eqs (53) and (54) into (61) gives:

$$\lambda_a \left[\frac{2\ a^{3/2}}{\mu^{1/2}\ (\pi-m)} \int_o \frac{(u + \lambda_2 \cos(f)\ df}{D^{1/2}} \right]$$

$$+ \lambda_i \left[\frac{a^{1/2}}{2\mu^{1/2}\ (\pi-m)} \int_o^g \frac{\cos^2(f+s)\ df}{D^{1/2}} \right] + 1 = 0 \qquad (62)$$

For this problem, Eq (56) becomes

$$\lambda_a \frac{\partial}{\partial u} \left[\frac{da}{d\tau} \right] + \lambda_i \frac{\partial}{\partial u} \left[\frac{di}{d\tau} \right] = 0 \qquad (63)$$

Solving for the partial derivative yields

$$\lambda_a \left[\frac{2\ a^{3/2}}{\mu^{1/2}\ (\pi-m)} \int_0 \frac{[\lambda_2^2 \sin^2(f) + \cos^2(f+s)]\ df}{D^{3/2}} \right]$$

$$- \lambda_i \left[\frac{2\ a^{1/2}}{\mu^{1/2}\ (\pi-m)} \int_0^g \frac{[u + \lambda_2 \cos(f)]\cos^2(f+s)\ df}{D^{3/2}} \right] = 0 \qquad (64)$$

For this problem, Eq (57) becomes

$$\lambda_a' = \frac{-\partial H}{\partial a} \qquad (65)$$

$$\lambda_i' = \frac{-\partial H}{\partial i} \qquad (66)$$

Expanding Eq (65)

$$\frac{\partial H}{\partial a} = \lambda_a \frac{\partial}{\partial a}\left[\frac{da}{d\tau}\right] + \lambda_i \frac{\partial}{\partial a}\left[\frac{di}{d\tau}\right] \qquad (67)$$

Recalling that s is a function of m and m is a function of both a and i,

$$\frac{\partial}{\partial a}\left[\frac{da}{d\tau}\right] = \left[\frac{\partial}{\partial a}\ \frac{da}{d\tau}\right] + \left[\frac{\partial}{\partial m}\ \frac{da}{d\tau}\right] \frac{\partial m}{\partial a} \qquad (68)$$

and

$$\frac{\partial}{\partial a}\left[\frac{di}{d\tau}\right] = \left[\frac{\partial}{\partial a}\ \frac{di}{d\tau}\right] + \left[\frac{\partial}{\partial m}\ \frac{di}{d\tau}\right] \frac{\partial m}{\partial a} \qquad (69)$$

Cass derives the contents of Eqs (68) and (69). Substituting Eqs (67) through (69) into (65) yields

$$\lambda_a' = -\lambda_a \left[\frac{a^{1/2}\,[3(\pi-m) + 2\,X\,a]}{\mu^{1/2}\,(\pi-m)^2} \int_o^g \frac{(u + \lambda_2\cos(f))\;\; df}{D^{1/2}} \right.$$

$$+ \frac{2\,X\,a^{3/2}}{\mu^{1/2}\,(\pi-m)^2} \int_o^g \frac{(u + \lambda_2\cos(f))\,\sin(f+s)\,\cos(f+s)\;\; df}{D^{3/2}}$$

$$\left. - \frac{4\,X\,a^{3/2}\,(u + \lambda_2\cos(2m))}{\mu^{1/2}(\pi-m)\,[\lambda_2^2\sin^2(2m) + 4(u+\lambda_2\cos(2m))^2 + \cos^2(s-2m)]^{1/2}} \right]$$

$$-\lambda_i \left[\frac{(\pi-m) + 2\,X\,a}{4\,\mu^{1/2}\,a^{1/2}\,(\pi-m)^2} \int_o^g \frac{\cos^2(f+s)\;\; df}{D^{1/2}} \right.$$

$$- \frac{X\,a^{1/2}}{\mu^{1/2}\,(\pi-m)} \int_o^g \frac{\sin(f+s)\,\cos(f+s)\;\; df}{D^{1/2}}$$

$$+ \frac{X\,a^{1/2}}{2\,\mu^{1/2}\,(\pi-m)} \int_o^g \frac{\sin(f+s)\,\cos^3(f+s)\;\; df}{D^{3/2}}$$

$$\left. - \frac{X\,a^{1/2}\;\cos^2(s-2m)}{\mu^{1/2}(\pi-m)\,[\lambda_2^2\sin^2(2m) + 4(u+\lambda_2\cos(2m))^2 + \cos^2(s-2m)]^{1/2}} \right] \tag{70}$$

where

$$X = \frac{G_o - F_o(a^2-1)^{-1/2}}{a^2\,[\cos^2(B) - \cos^2(\sigma_o)]^{1/2}} \tag{71}$$

In a similar manner, λ_i' can be found to be

$$\lambda_i' = -\lambda_a \left[\frac{2\,Y\,a}{\mu^{1/2}\,(\pi-m)^2} \int_o^g \frac{(u + \lambda_2\cos(f))\;\; df}{D^{1/2}} \right.$$

$$+ \frac{2\,Y\,a^{3/2}}{\mu^{1/2}\,(\pi-m)} \int_o^g \frac{(u + \lambda_2\cos(f))\,\sin(f+s)\,\cos(f+s)\;\; df}{D^{3/2}}$$

$$\left. - \frac{4\,Y\,a^{3/2}\,(u + \lambda_2\cos(2m))}{\mu^{1/2}(\pi-m)\;[\lambda_2^2\sin^2(2m) + 4(u+\lambda_2\cos(2m))^2 + \cos^2(s-2m)]^{1/2}} \right]$$

$$-\lambda_i \left[\frac{Y\,a^{1/2}}{2\,\mu^{1/2}\,(\pi-m)^2} \int_o^g \frac{\cos^2(f+s)\;\; df}{D^{1/2}} \right.$$

$$- \frac{Y^{1/2}a}{\mu^{1/2}\,(\pi-m)} \int_o^g \frac{\sin(f+s)\,\cos(f+s)\;\; df}{D^{1/2}}$$

$$+ \frac{Y\,a^{1/2}}{2\,\mu^{1/2}\,(\pi-m)} \int_o^g \frac{\sin(f+s)\,\cos^3(f+s)\;\; df}{D^{3/2}}$$

$$\left. - \frac{Y\,a^{1/2}\;\cos^2(s-2m)}{\mu^{1/2}(\pi-m)\;[\lambda_2^2\sin^2(2m) + 4(u+\lambda_2\cos(2m))^2 + \cos^2(s-2m)]^{1/2}} \right] \tag{72}$$

where

$$Y = \frac{-\cos(\sigma_o)\,\sin(B)\,\cos(\delta_o - i)}{\cos^2(B)\;\;[\cos^2(B) - \cos^2(\sigma_o)]^{1/2}} \tag{73}$$

Now, Eqs (62) and (64) can be solved simultaneously for λ_a and λ_i in terms of integrals containing the state and control variables. From Eq (64),

$$\lambda_i = \frac{\lambda_a\, a \displaystyle\int_o^g \frac{[\lambda_2^2 \sin^2(f) + \cos^2(f+s)]\ df}{D^{3/2}}}{\displaystyle\int_o^g \frac{(u + \lambda_2 \cos(f))\cos^2(f+s)\ df}{D^{3/2}}} \tag{74}$$

Substituting this result into Eq (62) gives

$$\lambda_a = \left[\frac{-1}{Q(u,s)}\right] \frac{2\,\mu^{1/2}\,(\pi-m)}{a^{3/2}} \int_o^g \frac{(u + \lambda_2\cos(f))\cos^2(f+s)\ df}{D^{3/2}} \tag{75}$$

where

$$Q(u,s) = \int_o^g \frac{4(u + \lambda_2\cos(f))\ df}{D^{1/2}} \int_o^g \frac{(u + \lambda_2\cos(f))\cos^2(f+s)\ df}{D^{3/2}}$$

$$+ \int_o^g \frac{\cos^2(f+s)\ df}{D^{1/2}} \int_o^g \frac{[\lambda_2^2 \sin^2(f) + \cos^2(f+s)]\ df}{D^{3/2}} \tag{76}$$

Eqs (74) and (75) can be substituted into either Eq (70) or (72) to also produce an integral equation in terms of the state and control variables. Using the new expression for Eqs (70) or (72), the two state Eqs (53) and (54), and equating Eq (36) to zero to find λ_2, the minimum time problem can be solved.

III. SOLUTION ALGORITHM

The solution to the minimum time problem uses dimensionless parameters. For instance, a is measured in DU's, τ is measured in DU's and TU's, the gravitational parameter μ is equal to 1 DU^3/TU^2, and all angles are measured in radians.

Choose either Eq (70) or (72) to use in the solution. In this solution, equation (70) is used. It might appear Eq (72) is less complicated since it has fewer terms and Y is a factor in all terms. Notice, λ_i is a constant when m = 0 and Y = 0. Cass revealed that in the range of interest for λ_i, u is double-valued (6:39). It was also found λ_i varied dramatically for different values of a and i. See Figures (6) and (7). Notice the λ_a curve maintains its shape and only changes slightly between initial and final conditions. The λ_i curve is not as well behaved. The fact u is double-valued for λ_i causes the search scheme to diverge. That is, for a particular value of λ_i , there could be two values of u. Which value of u is better and how can one use a numerical search scheme to find that u? To avoid this complication, equation (70) is used. Now, for a particular λ_a, there is only one value of u.

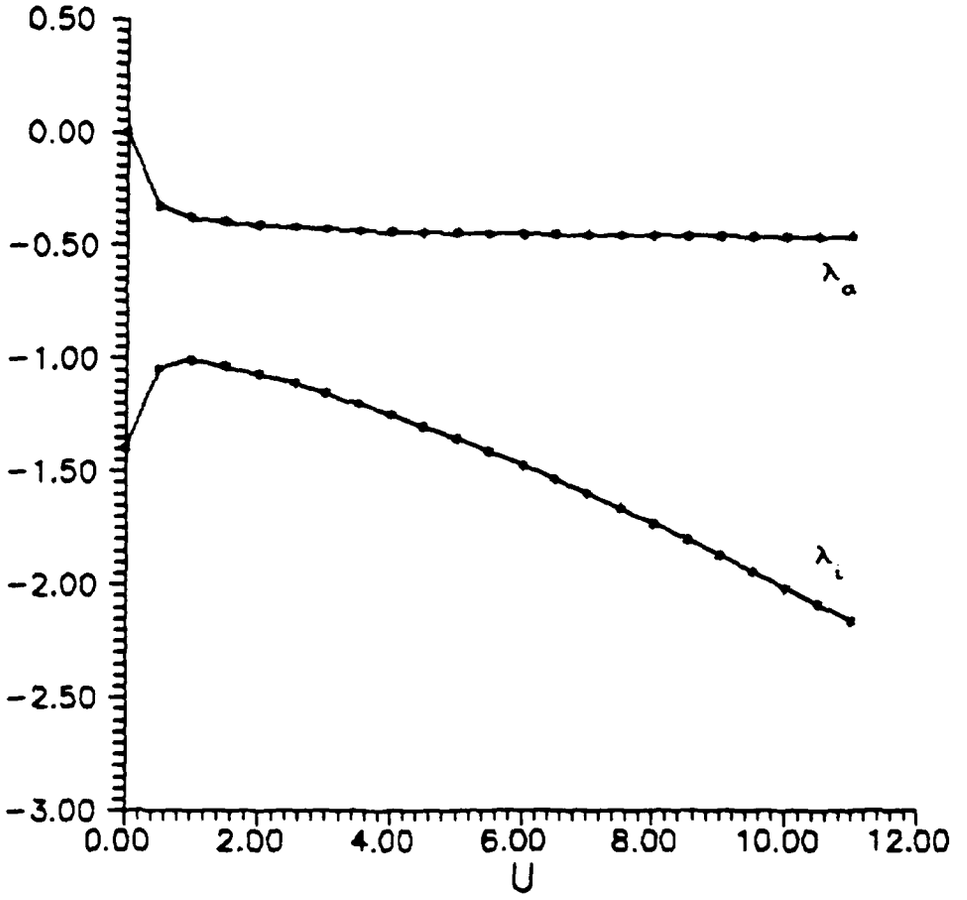

Figure 6. λ_a and λ_i for the First Day of Winter with a = 1.03 DU, i = 0.4974, and Ω = 180 degrees

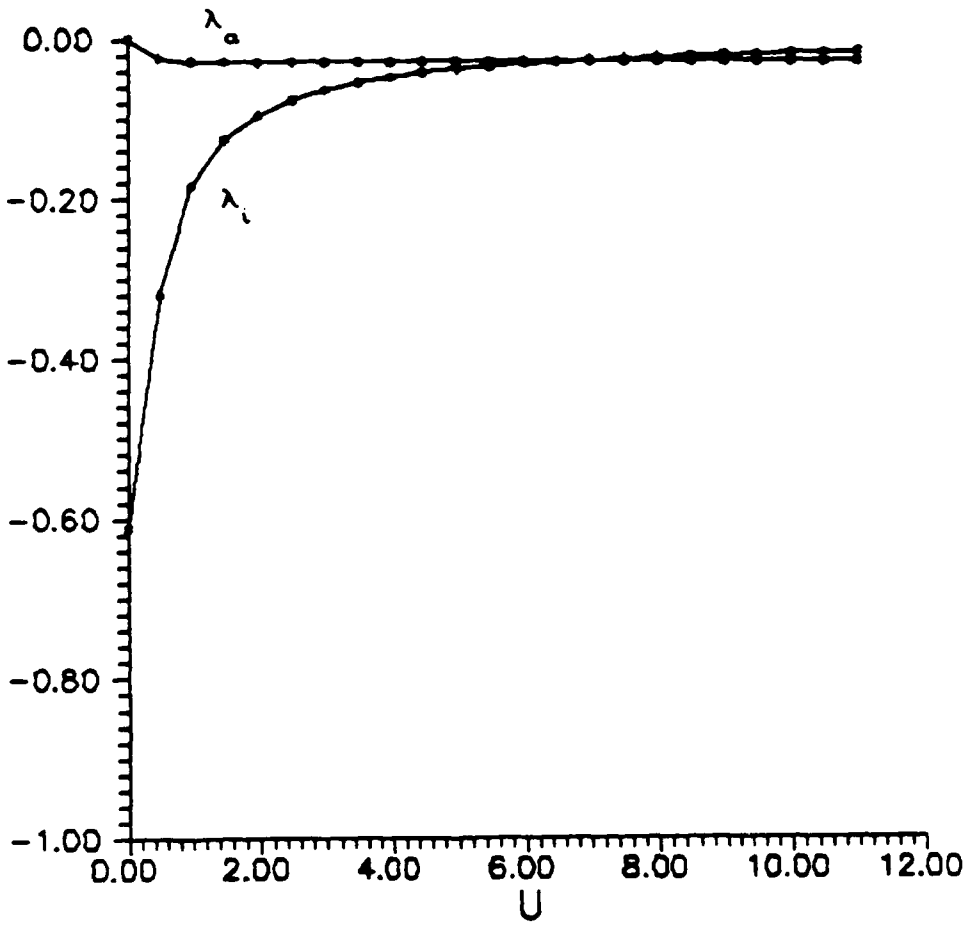

Figure 7. λ_a and λ_i for the First Day of Winter with a = 6.6 DU, i = 0.0, and Ω = 180 degrees

The minimum time solution is calculated in the following way:

1. Input initial boundary conditions.

   initial a = 1.03 DU

   initial i = 0.4974 rad (28.45 degrees)

2. Pick an initial value for λ_a ($\lambda_a(0)$). See Figures 8 through 12 for $\lambda_a(0)$ during the analyzed dates.

3. Determine sun-earth parameters

   input: a, i, Ω, day

   output: m, B, L, σ_o. Then calculate s and g.

4. Iterate equation (75) in order to find what u would produce that λ_a. See step 4a concerning λ_z in equation (75). NOTE: Simpson's rule was used to evaluate the integrals (5:165). Bisection method was used for the iteration of u (5:29).

   input: λ_a, s, g, m, a

   output: u, λ_i

4a. λ_z was calculated for each guess of u using the constraint $\Delta e = 0$ (Eq (36)). The bisection method was used to determine λ_z.

   input: u, s, g

   output: λ_z

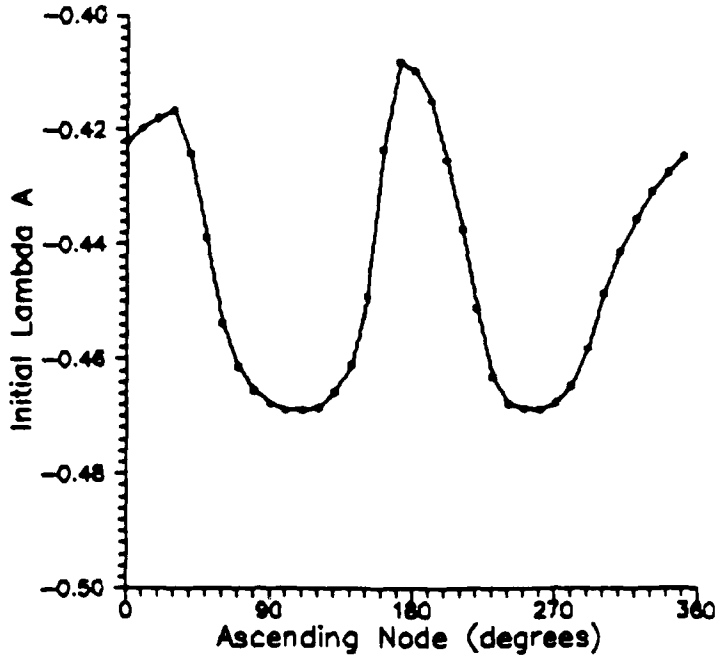

Figure 8. $\lambda_a(0)$ During the First Day of Winter

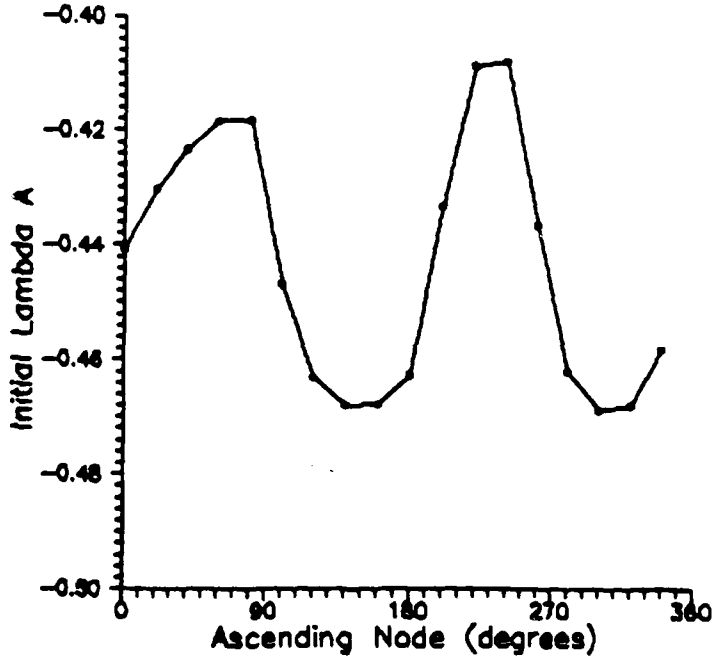

Figure 9. $\lambda_a(0)$ Midway Between Winter and Spring

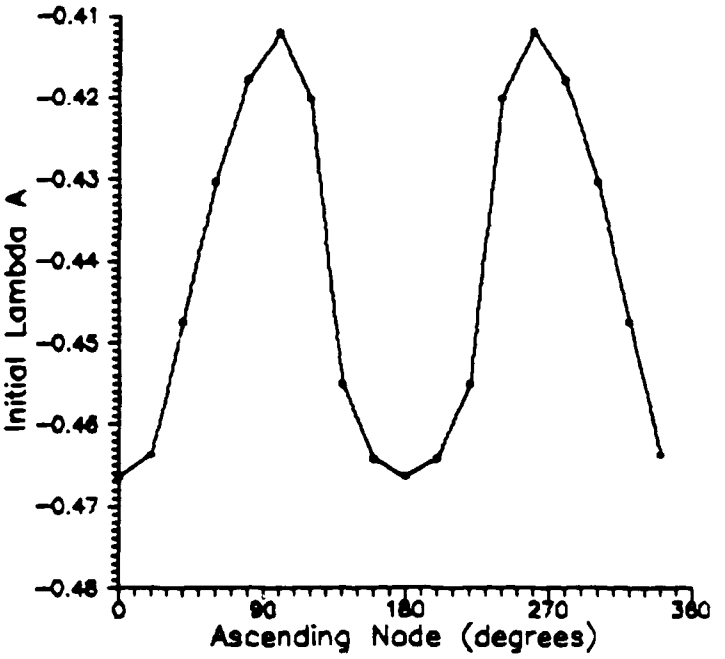

Figure 10. $\lambda_a(0)$ During the First Day of Spring

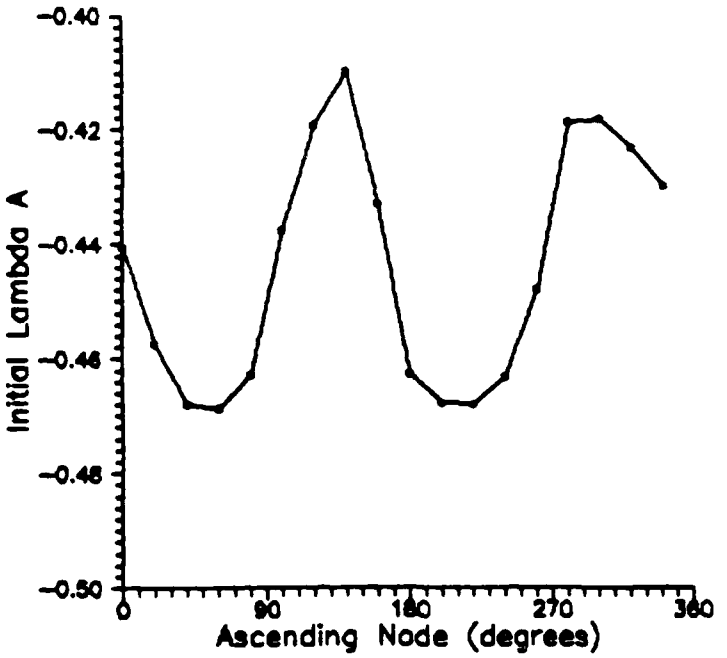

Figure 11. $\lambda_a(0)$ Midway Between Spring and Summer

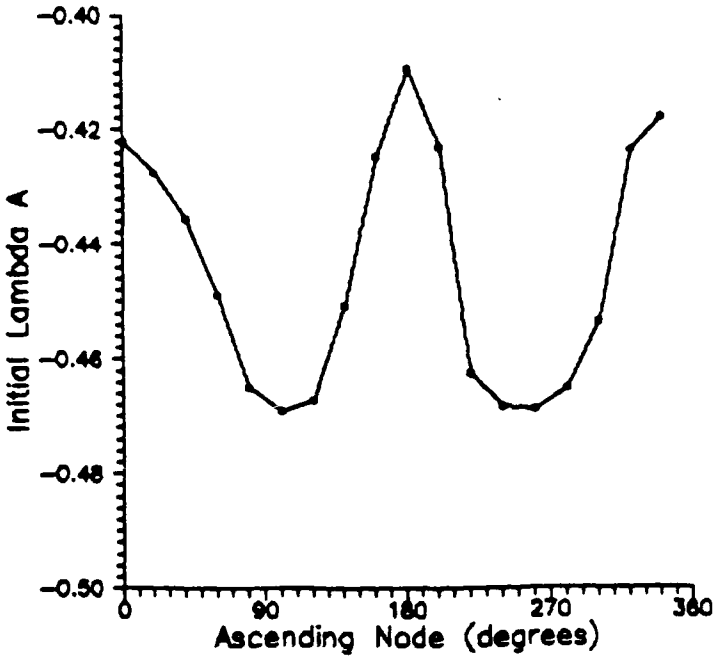

Figure 12. $\lambda_a(0)$ During the First Day of Summer

5. Since small changes in orbital elements:

new a = a + Δa

new i = i - Δi

where Δa and Δi are calculated using Eqs (53) and (54), respectively. These equations were not integrated since the changes are very small. To approximate the integration, $\Delta\tau$ was fixed at 0.01.

<u>input</u>: u, λ_2, a, m, s, g

<u>output</u>: Δa, Δi

6. Use Eq (70) to find the new λ_a

new $\lambda_a = \lambda_a + \Delta\lambda_a$

where

$$\lambda_a' = \frac{d\lambda_a}{d\tau} \approx \frac{\Delta\lambda_a}{\Delta\tau} = \text{rhs(right hand side) of Eq (70)}$$

then

$$\Delta\lambda_a = (\text{rhs})\ \Delta\tau$$

The rhs of Eq (70) uses the current value of a (not the new a calculated in step 5). $\Delta\tau$ = 0.01.

<u>input</u>: λ_a, λ_i, a, m, s, g, λ_2, G_o, F_o, B, σ_o, u

<u>output</u>: new λ_a

7. Check if met final boundary conditions where:

final a = 6.6 DU

final i = 0.0 radians

Use the flowchart for checking final boundary conditions:

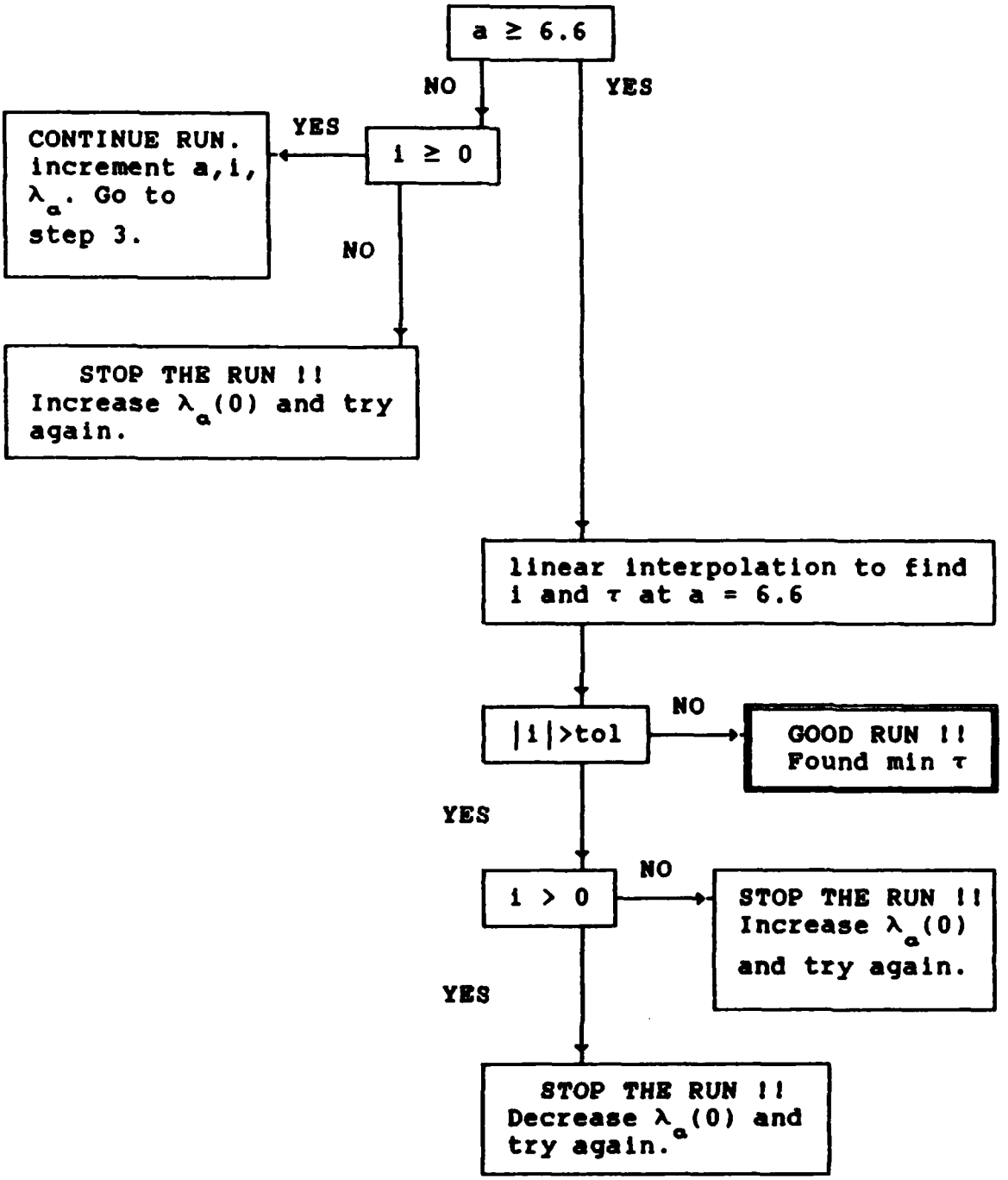

where tol = 0.001 radian

IV. RESULTS AND DISCUSSION

This study analyzes the transfer times for key dates during one-half of a year from the first day of winter to the first day of summer. The transfer times for the other half of the year are assumed to be similar to those of the analyzed dates. The analyzed dates are: first day of winter(21 DEC), midway between winter and spring(4 FEB), first day of spring(21 MAR), midway between spring and summer(6 MAY), and the first day of summer(21 JUN). The reference day used in the computer program is the vernal equinox, resulting in the analyzed day numbers to be 274, 320, 0, 46, and 91, respectively. A point should be made concerning the number of data points. The number of data points per day is chosen to yield general characteristics of the data and is not designed to give exact numerical quantities.

All transfers required the same change in the semi-major axis and inclination. The initial bounday conditions are a_i= 200 km = 1.03 DU and i_i= 28.5 degrees = 0.4974 radians (a possible shuttle orbit). The final boundary conditions are a_f = 6.6 DU and i_f = 0.0 radians. Recall the total accumulated velocity change (τ) is minimized rather than the actual transfer time. If one minimizes τ then transfer time is also minimized.

Figures 13 through 17 show how τ varied with Ω during each of the five analyzed days. Each plot of τ is a

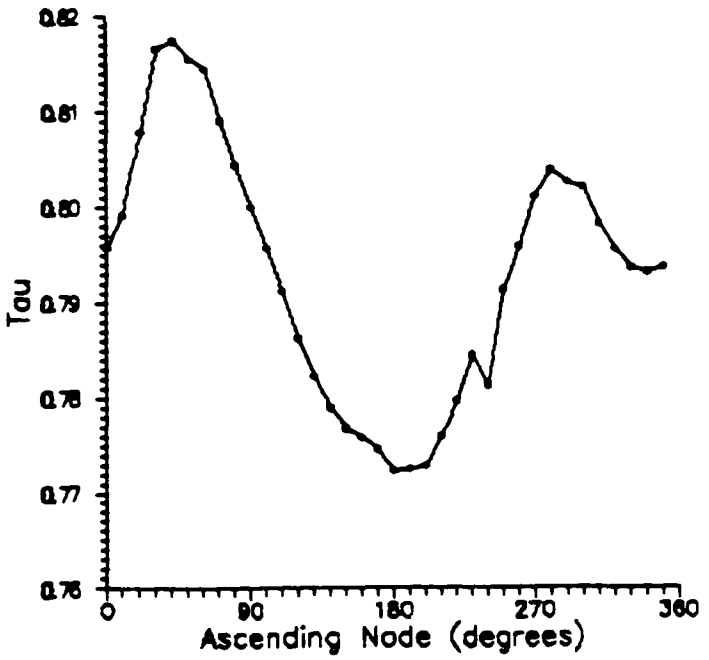

Figure 13. τ on the First Day of Winter

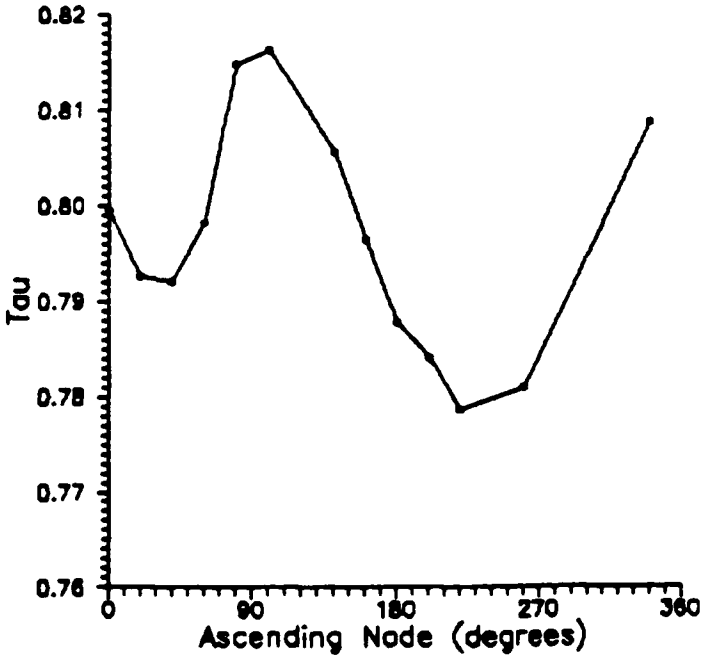

Figure 14. τ Midway Between Winter and Spring

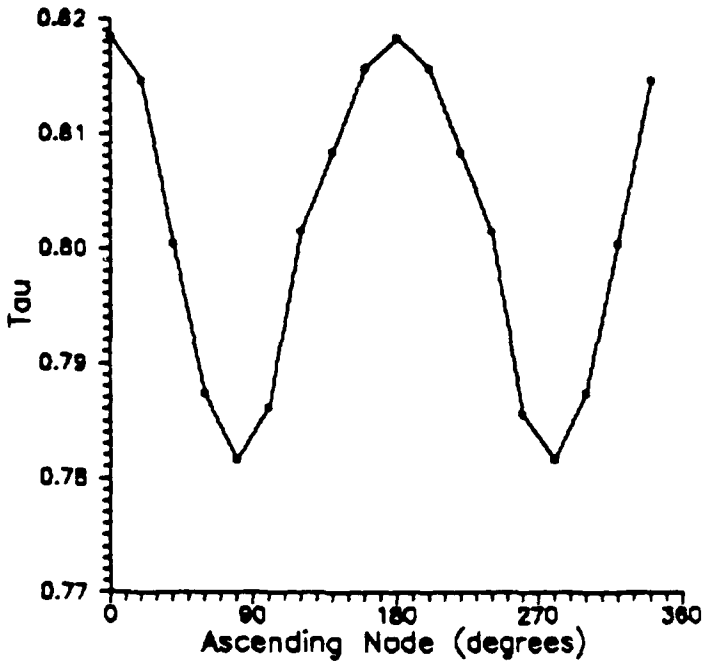

Figure 15. τ on the First Day of Spring

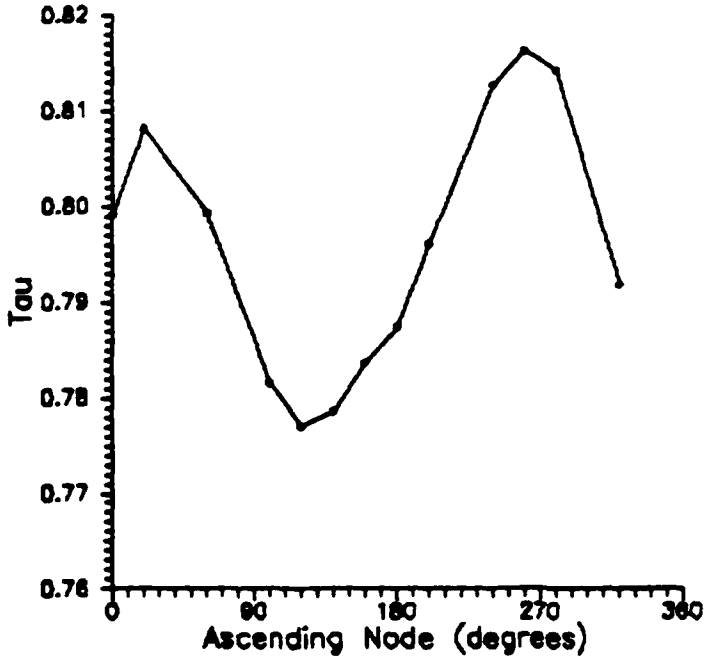

Figure 16. τ Midway Between Spring and Summer

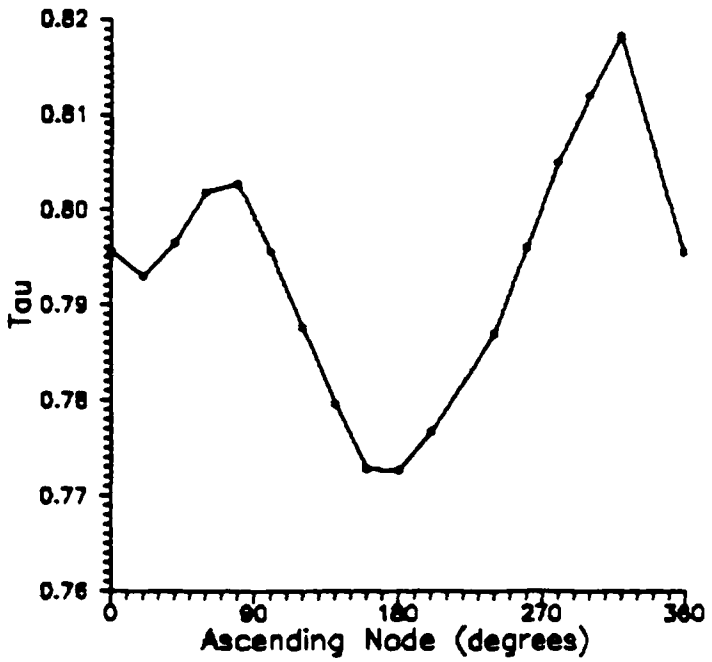

Figure 17. τ on the First Day of Summer

"sinusoid" of sorts and varies in a predictable manner. The plot for spring (Figure 15) is symmetric for τ. The minimum τ on each day in Figures 13 through 17 is plotted versus the day in Figure 18. The ascending node at which the minimum τ's occurred are also plotted versus the day in Figure 19. The following paragraphs will examine Figures 13 through 19.

An important trend arises concerning the optimal ascending node in Figures 13 through 17. Note: the optimal ascending node is defined as the ascending node where τ is a minimum. The line of nodes (a line connecting the ascending and descending node) for the minimum τ orbit on each day is perpendicular to, or nearly perpendicular to, the earth-sun line. A comparison of Figures 13 through 17 and 20 through 24 indicates the optimal launch time (i.e., acsending node) is the one which minimizes the time in the earth's shadow. Figures 20 through 24 show the ascending node for the quickest escape of the earth's shadow occurred at, or very near, the ascending node for the minimum τ orbit. The ascending node for the minimum initial shadow half-angle (m_o) also corresponds to the minimum τ orbit. Obviously, the less time spent in the earth's shadow allows more thrusting time per orbit. More thrusting time per orbit yields smaller transfer times.

Assuming the minimum τ orbit requires the line of node to be perpendicular to the earth-sun line, the question remains

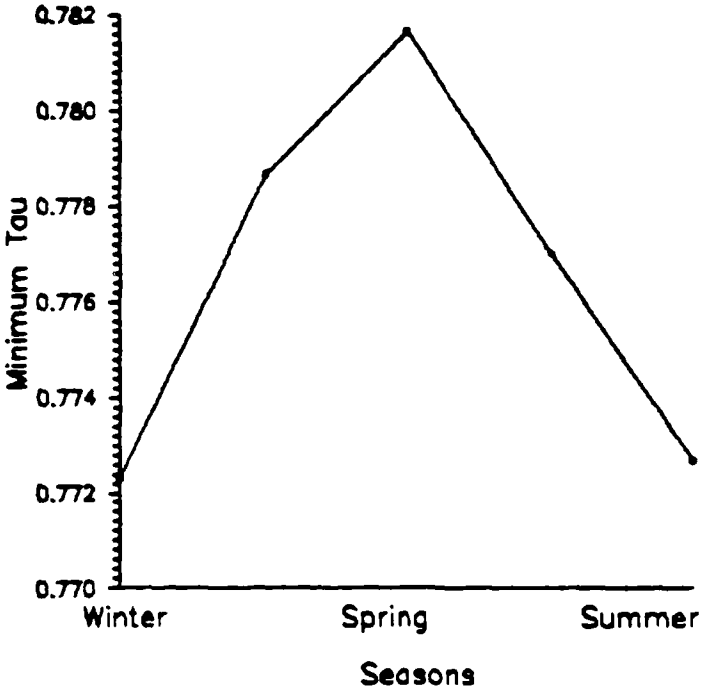

Figure 18. Variation of Minimum τ During the Year

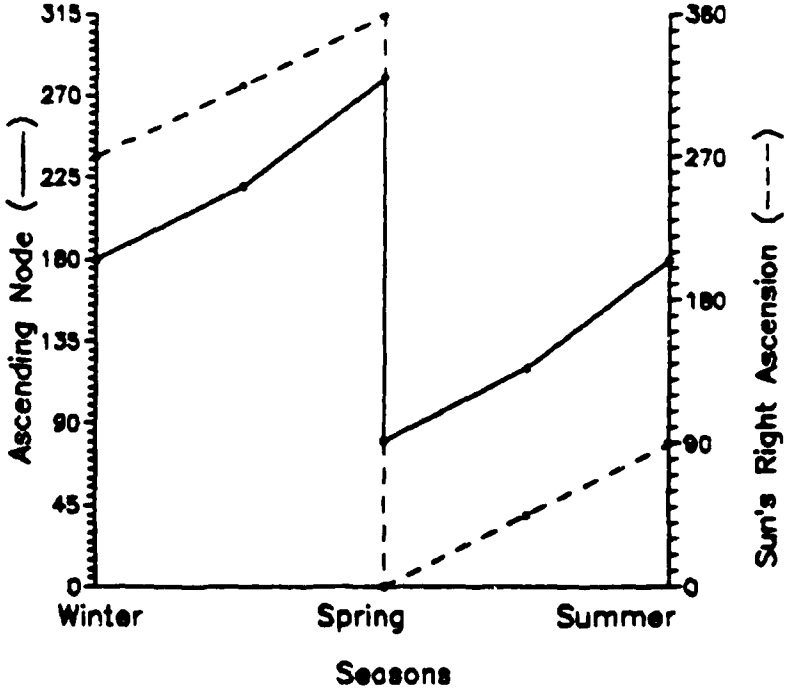

Figure 19. Variation of Ω at Minimum τ and $\alpha_{\odot}$ During the Year

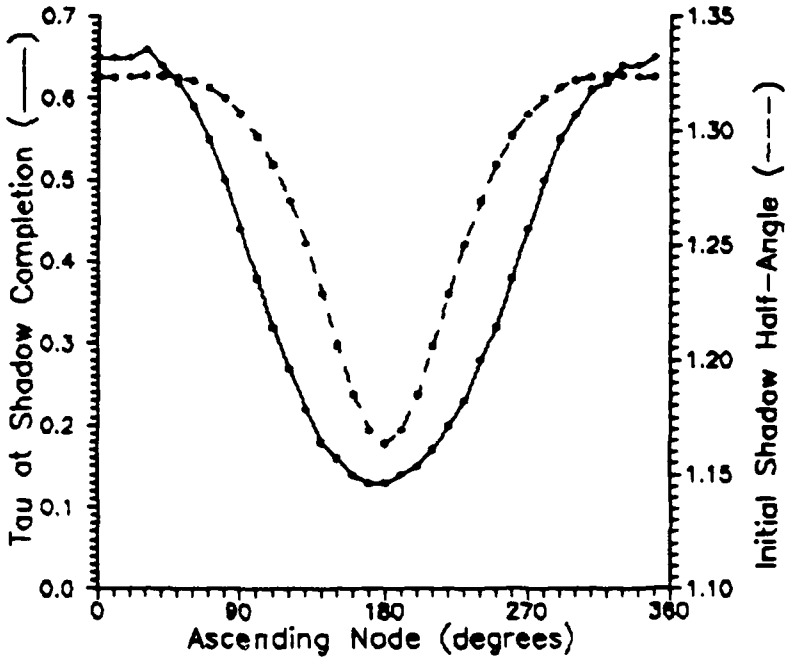

Figure 20. Effects of Ω on m During the First Day of Winter

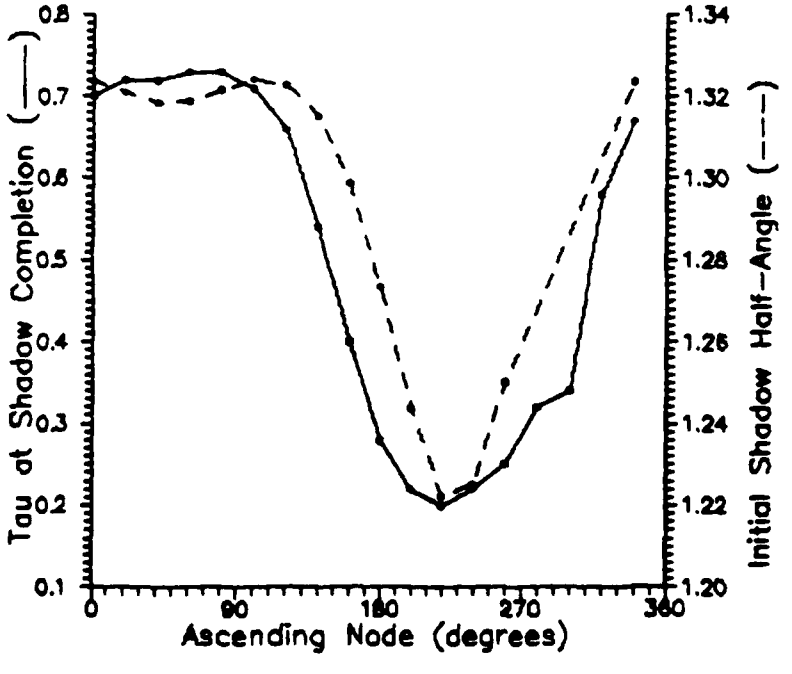

Figure 21. Effects of Ω on m Midway Between Winter and Spring

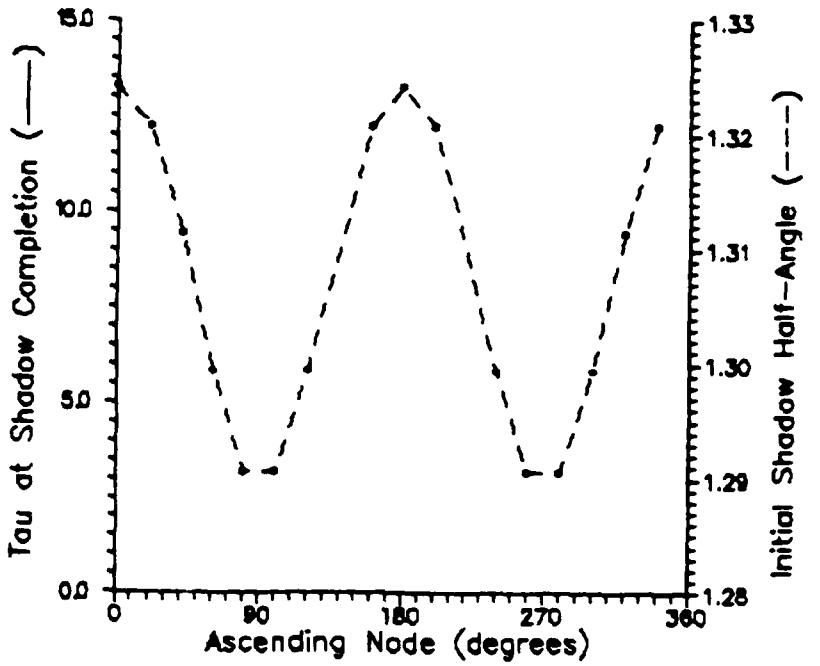

Figure 22. Effects of Ω on m During the First Day of Spring

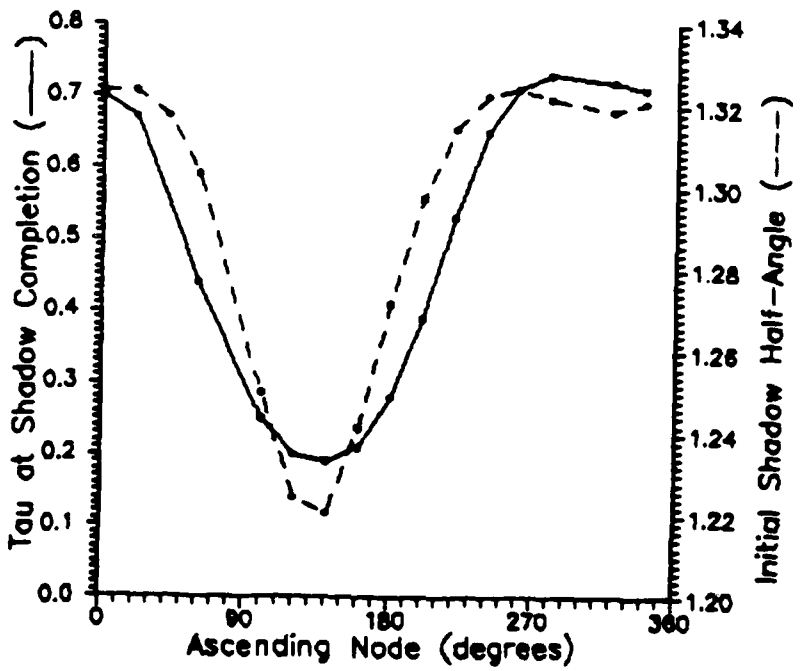

Figure 23. Effects of Ω on m Midway Between Spring and Summer

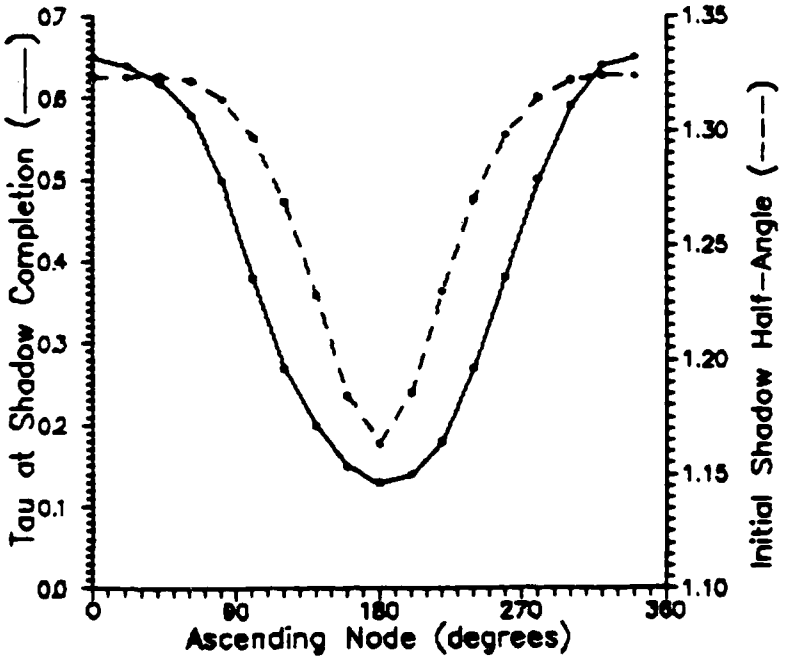

Figure 24. Effects of Ω on m During the First Day of Summer

as to which node is the ascending node. If the northern hemisphere is between fall and spring, then the ascending node is ($\alpha_\odot - \pi/2$). If the northern hemisphere is between spring and fall, then the ascending node is ($\alpha_\odot + \pi/2$). For the first day of spring and fall, the optimal ascending node is both ($\alpha_\odot \pm \pi/2$). These orientations will minimize m_o, thereby minimizing τ. Figure 19 shows how the ascending node at minimum τ changed with respect to the day of the year. The right ascension of the sun is also included in Figure 19 for comparison purposes. The two optimal ascending nodes for spring is due to the symmetric lighting conditions.

Another trend in the data is the change in semi-major axis (Δa) is greater than the change in inclination (Δi) during the initial phase of the transfer. Figure 25 displays a typical profile for Δa and Δi. This agrees with the fact that plane changes require much more energy than coplanar changes when gravity is a major factor (1, 2:169-170). This profile is also the path needed by the spacecraft to minimize or eliminate (depending on the time of year) the time in the earth's shadow.

Figure 18 shows the overall minimum τ orbit occurring at both the first day of summer and the first day of winter. This corresponds with the overall minimum m_o which is plotted in Figure 26. The difference between the τ's in Figure 6 is only 1.21%. Whereas the change in m_o's in Figure 26 is 10.91%. However, these differences in τ and m_o are not

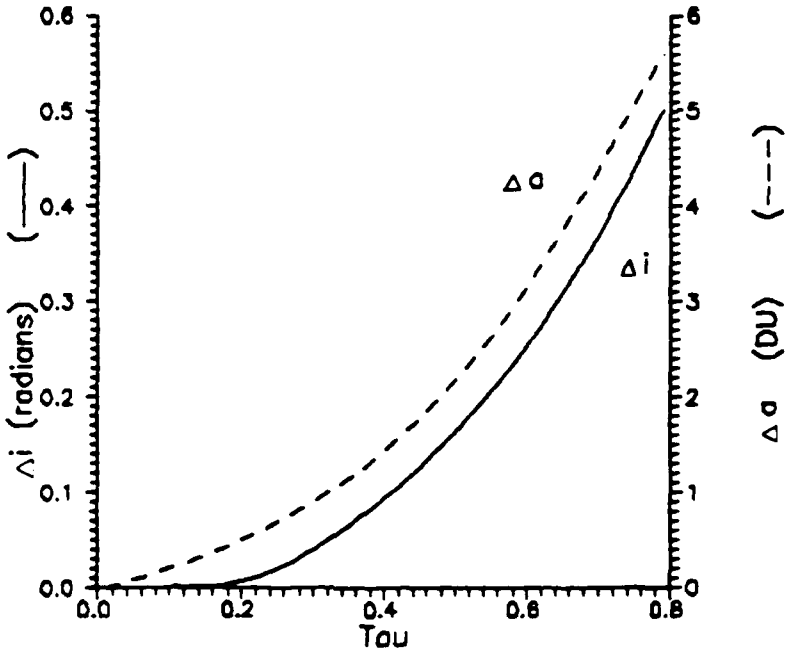

Figure 25. Propagation of a and i During an Orbit Transfer on 4 FEB 88 with Ω = 180 degrees

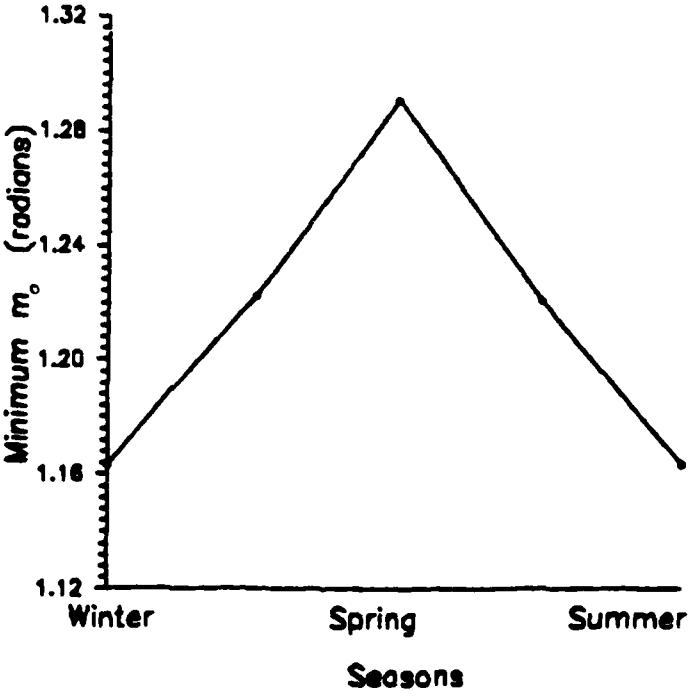

Figure 26. Variation of Minimum m_o During the Year

consistent on any particular day (Figures 13 through 17 and 20 through 24). For instance, τ varied from 4.7% to 5.9% on any of the analyzed dates. Whereas m_o varied from 2.6% to 13.8%. The upper limit of these changes for τ and m_o occurred simultaneously; as did the lower limit. Table I contains the minimum and maximum values of τ and m_o for the analyzed dates.

TABLE I. Changes in τ and m_o

Date (day#)	min / max τ (DU/TU)	min / max m_o (radians)	% change in τ	% change in m_o
21 DEC (274)	0.77232 0.81745	1.163663 1.324214	5.80	13.80
4 FEB (320)	0.77865 0.81628	1.222310 1.324079	4.83	8.32
21 MAR (0)	0.78165 0.81850	1.290653 1.324239	4.71	2.60
6 MAY (42)	0.77683 0.81626	1.220574 1.324144	5.07	8.49
21 JUN (91)	0.77268 0.81823	1.163673 1.324218	5.90	13.80

V. CONCLUSIONS AND RECOMMENDATIONS

This study determined the optimal launch time for a discontinuous, low thrust orbit transfer. The optimal launch times are the first day of winter and summer and occurred simultaneously with minimum m_o (smallest initial shadow half-angle). The actual transfer time in seconds is not calculated because the independent variable was changed from t to τ (the accumulated velocity change). This was done in order to analyze the entire class of low thrust rockets. If one wants to calculate the transfer time in seconds for a specific rocket, then use Eq (51) or (52) to change the independent variable from τ to t. If the independent variable is t, then the changes in $\alpha_\odot$ and $\delta_\odot$ during the transfer should be taken into account.

The following is a rough calculation for converting from τ to t. Solve for t using Eq (52)

$$t = \frac{1}{\dot{m}_p} \left[1 - \exp(-\tau \dot{m}_p / T_o) \right]$$

where

$$T_o = \frac{\text{thrust force}}{\text{vehicle mass}} = \frac{F}{m_{veh}}$$

$$\dot{m}_p = \frac{\text{propellant mass flow}}{\text{vehicle mass}} = \frac{\dot{m}}{m_{veh}}$$

As an example, use the engine parameters given in Ref 11:

$$F = 0.8 \text{ lb}$$

$$\dot{m} = 0.001 \text{ lb/sec}$$

with a payload of 10,000 lb (a large payload). Assume the total vehicle weight (including payload) is 14,000 lb. Then

$$T_o = \frac{F}{m_{veh}} = \frac{0.8 \text{ lb}}{14000 \text{ lb} / 32.2 \text{ ft/sec}^2} = 1.84 \times 10^{-3} \text{ ft/sec}^2$$

$$\dot{m}_p = \frac{\dot{m}}{m_{veh}} = \frac{0.001 \text{ lb/sec}}{14000 \text{ lb}} = 7.14 \times 10^{-8} \text{ /sec}$$

$$\tau_{min} = 0.77232 \text{ DU/TU} * \frac{2.093 \times 10^7 \text{ ft}}{1 \text{ DU}} * \frac{1 \text{ TU}}{806.8 \text{ sec}}$$

$$= 20{,}035 \text{ ft/sec}$$

Substituting yields t = 7,568,926 sec = 2102 hr = 88 days. Using τ_{max} of 0.8185 DU/TU yields t = 91 days; a 3.9% increase in transfer time.

As a continuation to this study, one could find the optimal launch time without constraining Δe to be equal to zero. Another topic of interest is to take into account a non-spherical earth, thereby causing a regression in the line of nodes and rotation of the line of apsides (if orbit is eccentric).

Bibliography

1. Alfano, Capt Salvatore. Low Thrust Orbit Transfer. MS thesis, AFIT/GA/AA/82D-1. School of Engineering, Air Force Institute of Technology (AU), Wright-Patterson AFB OH, December 1982.

2. Bates, Roger R., Donald D. Mueller, and Jerry E. White. Fundamental of Astrodynamics. New York: Dover Publications, 1971.

3. Brewer, George R. Ion Propulsion. New York: Gordon and Breach Science Publishers, 1970.

4. Bryson, Arthur E., Jr. and Yu-Chi Ho. Applied Optimal Control. New York: Hemisphere Publishing, 1975.

5. Burden, Richard L. and Douglas J. Faires. Numerical Analysis (Third Edition). Boston: Prindle, Weber, and Schmidt, 1985.

6. Cass, Capt John R., Jr. Discontinuous Low Thrust Orbit Transfer. MS thesis, AFIT/GA/AA/83D-1. School of Engineering, Air Force Institute of Technology (AU), Wright-Patterson AFB OH, December 1983.

7. Finke, Robert C. "Electric Propulsion and Its Applications to Space Missions, "Progress in Astronautics and Aeronautics, 79: xi-xx (1981).

8. Leitmann, George. Optimization Techniques: With Applications to Aerospace Systems. New York: Academic Press, 1962.

9. Link, Frantisek. Eclipse Phenomena in Astronomy. New York: Springer-Verlag, 1969.

10. Marec, J.P. Optimal Space Trajectories. New York: Elsevier Scientific Publishing Co., 1979.

11. Scott, William B. "USAF Pursues Development of Solar-Powered Rocket," Aviation Week and Space Technology, 119-120 (19 OCT 87).

12. Wiesel, William E, Jr. Class notes for MECH 636, Advanced Astrodynamics. School of Engineering, Air Force Institute of Technololgy (AU), Wright-Patterson AFB OH, Winter Quarter 1988.

Vita

Jeffrey Michael McCann was born on [redacted] in [redacted] He graduated from Churchill Area High School, [redacted] He attended The Pennsylvania State University and graduated with a degree in Aerospace Engineering in 1984. He received a commission through USAF Officers Training School in August 1984. He then served at the Foreign Technology Division at Wright-Patterson AFB, Ohio before entering the School of Engineering at the Air Force Institute of Technology, Wright-Patterson AFB, Ohio in June 1987.

[redacted]

UNCLASSIFIED
SECURITY CLASSIFICATION OF THIS PAGE

REPORT DOCUMENTATION PAGE

Form Approved OMB No. 0704-0188

1a. REPORT SECURITY CLASSIFICATION: UNCLASSIFIED	1b. RESTRICTIVE MARKINGS
2a. SECURITY CLASSIFICATION AUTHORITY	3. DISTRIBUTION / AVAILABILITY OF REPORT: Approved for public release; distribution unlimited.
2b. DECLASSIFICATION / DOWNGRADING SCHEDULE	
4. PERFORMING ORGANIZATION REPORT NUMBER(S): AFIT/GA/AA/88D-7	5. MONITORING ORGANIZATION REPORT NUMBER(S)
6a. NAME OF PERFORMING ORGANIZATION: School of Engineering; 6b. OFFICE SYMBOL (If applicable): AFIT/ENY	7a. NAME OF MONITORING ORGANIZATION
6c. ADDRESS (City, State, and ZIP Code): Air Force Institute of Technology (AU) Wright-Patterson AFB, Ohio 45433-6583	7b. ADDRESS (City, State, and ZIP Code)
8a. NAME OF FUNDING / SPONSORING ORGANIZATION; 8b. OFFICE SYMBOL (If applicable)	9. PROCUREMENT INSTRUMENT IDENTIFICATION NUMBER
8c. ADDRESS (City, State, and ZIP Code)	10. SOURCE OF FUNDING NUMBERS: PROGRAM ELEMENT NO. / PROJECT NO. / TASK NO / WORK UNIT ACCESSION NO.

11. TITLE (Include Security Classification)

OPTIMAL LAUNCH TIME FOR A DISCONTINUOUS LOW THRUST ORBIT TRANSFER(UNCLASSIFIED)

12. PERSONAL AUTHOR(S)
Jeffrey M. McCann, Capt, USAF

13a. TYPE OF REPORT	13b. TIME COVERED	14. DATE OF REPORT (Year, Month, Day)	15. PAGE COUNT
MS Thesis	FROM _____ TO _____	88 DEC	65

16. SUPPLEMENTARY NOTATION

17. COSATI CODES			18. SUBJECT TERMS (Continue on reverse if necessary and identify by block number)
FIELD	GROUP	SUB-GROUP	
22	03		low thrust, electric propulsion, orbit transfer, solar propulsion, transfer trajectories.

19. ABSTRACT (Continue on reverse if necessary and identify by block number)

Thesis Advisor: William E. Wiesel, Ph.D.

12 Jan 1989

20. DISTRIBUTION / AVAILABILITY OF ABSTRACT: ☒ UNCLASSIFIED/UNLIMITED ☐ SAME AS RPT. ☐ DTIC USERS	21. ABSTRACT SECURITY CLASSIFICATION: UNCLASSIFIED
22a. NAME OF RESPONSIBLE INDIVIDUAL: William E. Wiesel, Ph.D., Professor	22b. TELEPHONE (Include Area Code): (513) 255-4476; 22c. OFFICE SYMBOL: AFIT/ENY

DD Form 1473, JUN 86 — Previous editions are obsolete. — SECURITY CLASSIFICATION OF THIS PAGE: UNCLASSIFIED

Block 19 Continued.

This ~~study~~ searches for the optimal launch time of a discontinuous, low thrust transfer between non-coplanar, circular orbits. The spacecraft is assumed to be a solar-powered rocket that cannot provide thrust in the earth's shadow.

Two timescales are used to calculate a minimum time trajectory. The fast timescale produces a control law which maximizes a change in orbital elements for a single orbit. The slow timescale incorporates the control law so that the final boundary conditions are met in minimum time. Minimum transfer times are determined between winter and summer.